

Enhance Functionality of Titanium Dioxide Nanotube Arrays for Photo catalytic Degradation of Methylene Blue under Visible Light with Deposited Gold Nanoparticles

Areeya Aeimbhu and Atipol Sawang-arom

Department of Physics, Faculty of Science, Srinakharinwirot University, Bangkok, Thailand

Abstract: *Highly ordered and vertically aligned titanium dioxide nanotubes were productively prepared by in situ growth on titanium sheet by anodized titanium, processing a high surface-to-volume ratio with controllable dimensions. Gold nanoparticles (Au NPs) were subsequently deposited on the titanium dioxide nanotube arrays (TNAs) by electroplating technique. The microstructures of Au NPs/TNAs including surface chemical composition and surface area were studied with Field emission electron microscopy (FE-SEM), Energy Dispersion X-ray Spectroscopy (EDS), X-ray Photoelectron Spectroscopy (XPS), N₂ adsorption-desorption isotherm analysis (BET). The photo catalytic degradation of methylene blue over the visible light region of Au NPs/TNAs has been investigated and compared with the titanium sheet and TNAs. Photo degradation results demonstrated that photo catalytic activity of Au NPs/TNAs exhibited better photo catalytic performance under visible light irradiation compared to titanium sheet and TNAs in terms of percentage degradation of methylene blue. Between the photo catalysis kinetics model with first-order and second-order model; the second-order kinetic model was found to well present the experiment data of all catalysts. These results suggested that noble metal modification is a promising way to improve photo catalysts with both high activity and visible light sensitivity.*

Index Terms - photo catalytic, titanium dioxide nanotube arrays, gold nanoparticles, methylene blue.

I. INTRODUCTION

Since the discovery of photochemical decomposition of water under light irradiation into hydrogen and oxygen with titanium dioxide by Fujishima and Honda in 1972 [1], titanium dioxide has been investigated in the field of environmental remediation such as the treatment of waste water and degradation of organic molecules [2,3]. As a consequence of the presence of nanotube architecture, the surface area should be increased significantly due to their external and internal surfaces and one-dimensional nanostructures provides excellent electron pathways for charge transfer between interfaces. The limitation of titanium dioxide as a photo catalyst is its wide band gap (3.2 eV for anatase) which allows the creation of an electron-hole (e⁻h⁺) pair only when irradiated by ultraviolet (UV) light, a small fraction of the solar spectrum emission. Many different approaches were taken in order to overcome this problem,

such as using noble metal deposition, metal ion loading, cationic and anionic doping and sensitization TiO₂ with colour inorganic or organic compounds. Many endeavors to enhance the overall effective photo catalytic process for the visible light region. The deposition of Au NPs on TNAs substrate has been reported to enlarge the optical absorption of this material to visible spectral region due to a surface plasmon resonance (SPR) [4-15]. Here, the experiment attempted to deposit Au NPs on TNAs for photo catalytic degradation process using simple and low cost anodisation and electroplating technique. TNAs were formed in an electrolyte solutions contained ammonium fluoride and ethylene glycol. Then deposition of Au NPs carried out under galvanostatic conditions from an acid bath containing KAu(CN)₂ and various techniques have been used to characterize as-prepared samples. Moreover, the photo catalytic activity of as-prepared samples was studied by the degradation of methylene blue under visible light irradiation.

II. MATERIALS AND METHODS

A. Preparation of surface of titanium sheet.

Commercially pure titanium sheet (grade 2) was purchased from Prolog Titanium Co., Ltd. The titanium sheet was mounted in a cold mounting resin so that only one face of it exposed to the electrolyte. The exposed metal surface (area: 1 cm²) of each specimen was ground with silicon carbide abrasive papers (Buehler) from 120, 200, 600, 1000, 1200, 2000 and 2500 grade respectively. The surface of sheet was sequentially polished to a mirror finished with aqueous alumina (Al₂O₃) 5, 1, 0.3 and 0.05 micron (Buehler, Alpha Micro polish II). Afterward it was cleaned with acetone (Carlo Erba) in ultrasonic bath.

B. In situ growth titanium dioxide nanotube arrays (TNAs) via anodisation process on titanium sheet.

An electrochemical cell, the titanium sheet was placed as the anode with a graphite cathode. Using a DC power supply (KMB 3002), a constant potential of 20 volts was applied to run the process at room temperature (25°C) for a period of 100 minutes in electrolyte solutions which contained 0.3 wt%

of NH₄F (Carlo Erba), 10 wt% deionised water and ethylene glycol (Carlo Erba) [16].

C. Deposition of Gold nanoparticles (Au NPs) onto TNAs by electroplating technique

After anodising of a titanium sheet, the Au NPs was deposited onto TNAs substrates via electroplating procedure which involved the following steps: (1) a titanium sheet and a stainless steel plate was clipped onto the electrodes of a power supply and positioned in parallel with an interspacing of 3.0 cm; (2) the electrodes were soaked in KAu(CN)₂ electrolyte solution; (3) the electroplating potential and initial current were set to 5 volts and 4.5 mA/cm², respectively; (4) The samples were rinsed with deionised water and then dried in air.

D. Morphology and Spectroscopic Characterization.

The surface morphology of the prepared samples were observed by Field Emission Scanning Electron Microscope (FE-SEM: JEOL 6301F) and the elemental composition analysis were performed by means of Energy Dispersion X-ray Spectroscopy (EDS). Chemical state analysis was conducted with an X-ray Photoelectron Spectroscopy (XPS, AXIS Ultra DLD). A monochromatic Al source operating at 150 W with a pass energy of 80 eV and a step of 1.0 eV was used. Specific surface area analysis was done using the Brunauer, Emmett, and Teller (BET) method based on N₂ adsorption-desorption at 200°C (Autosorb 1C, Quantachrome, USA) with a NOVA 1000 series analyser. The reflectance diffusion spectrum (UV-Vis DRS) was obtained using a UV-Vis DRS: Agilent carry 5000. The concentration of methylene blue in the solution was determined from the absorbance at λ = 664 nm with that of the initial MB solution measured by a UV-visible absorption spectrometry (Lambda 25).

E. Photo catalytic degradation of Methylene blue (MB).

The photo catalytic activity of the prepared samples were analysed by photo catalytic decomposition of methylene blue, a representative of organic dyes in textile effluents, which considered as a model contaminant in the purification of dye waste water [17]. Methylene blue is a heterocyclic aromatic compound with analytical reagent grade (Gammaco). The accurate weighted quantity of the methylene blue was dissolved in deionised water to prepare the stock solution. Methylene blue concentration was determined using absorbance value measured before and after the irradiation with UV-Visible Spectrometer (Lambda 25). The photo catalytic reaction was performed under visible light irradiation using 20 watts compact fluorescent lamp (Philips, 65 lm/W, Luminous flux = 1150 lm, emission band in the visible region at 400-700 nm). The initial concentration of methylene blue was 26 mM in a beaker with a volume of 10 mL at room temperature (25°C). The prepared samples were immersed in methylene blue solution to stay in the dark without visible irradiation for 30 minutes to allow the system to reach an adsorption-desorption equilibrium, and then the visible light was turned on at different time interval (1-48

hours). After requested time for photo degradation, the relative concentration of methylene blue in the solution was determined through UV-Vis spectroscopy by comparing the 664 nm adsorption with the initial concentration of a methylene blue solution. Blank samples were also treated in same routine for the purpose of comparison. All experiments were repeated. The percentage degradation process was calculated based on equation [18,19]:

$$\% \text{Degradation} = \left(\frac{C_0 - C}{C_0} \right) \times 100 \quad (1)$$

Where C₀ is initial concentration of MB solution, C is concentration of methylene blue after photo irradiation.

The kinetic of photo catalytic oxidation follows Langmuir-Hishelwood (L-H) kinetic equation could be reduced to a pseudo first-order kinetic model equation [20]:

$$r = - \frac{d[C]}{dt} = k_1 [C] \quad (2)$$

If conversion efficiency is defined as

$$r = \frac{C}{C_0}$$

then equation (2) gives

$$\ln \left(\frac{C_0}{C} \right) = k_1 t \quad (3)$$

Where k₁ is the rate constant of the pseudo first-order model, r is degradation rate, C₀ is initial concentration of methylene blue and C is the MB concentration at time t.

The pseudo second-order kinetic model is expressed as

$$\frac{1}{C} = \frac{1}{C_0} + k_2 t \quad (4)$$

Where k₂ is the rate constant of the pseudo second-order model, C₀ is initial concentration of methylene blue and C is the methylene blue concentration at time t.

III. RESULTS

A. Surface area and pore size

The BET specific surface area of titanium sheet, TNAs and Au NPs/TNAs were given in Table 1. The BET specific area of TNAs and Au NPs/TNAs was higher to the titanium sheet. The deposition of Au NPs onto TNAs resulted in increase of BET surface and pore volume.

Table 1: BET surface area of each catalyst

Samples	Specific surface area (m ² /g)	Total pore volume (cc/g)
Titanium sheet	6.44	3.461×10 ⁻³
TNAs	35.83	2.216×10 ⁻²
Au NPs/TNAs	505.10	1.381×10 ⁻²

B. Morphology and composition analysis

Fig.1 demonstrated FE-SEM image of the machined-polished titanium sheet surface. The image

presented a characteristic of smooth surface without any scratches and residual during the polishing procedures which has led to mirror finish. The examination of titanium sheet by EDS technique has confirmed the presence of titanium with no impurities.

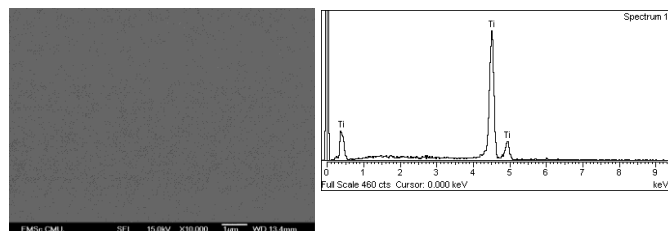
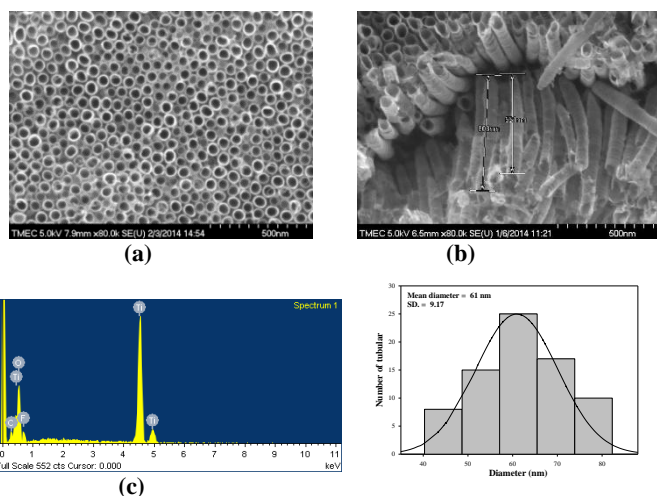


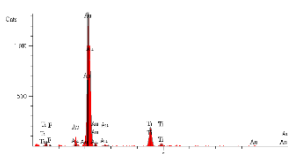
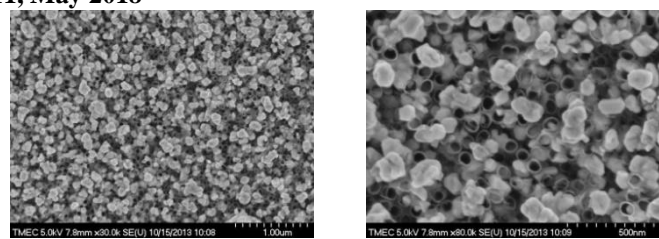
Fig. 1: FE-SEM top-view image of titanium sheet surface after polishing procedures and element analysis with EDS probe on machined-polished titanium surface.

Fig. 2(a) showed the FE-SEM image of the TNAs on titanium sheet. TNAs have tubular and uniform architecture. The lengths of the nanotubes ranged from 500-600 nm (Fig. 2(b)). The EDS element analysis (Fig. 2 (c)) exhibited significant peaks of titanium, carbon and oxygen. The EDS displays amounts of fluorine due to anodisation procedure. A mean inner diameter as estimated from the FE-SEM image was 61 nm (Fig. 2 (d)).



(d)
Fig. 2: Illustrative (a) top and (b) cross-sectional FE-SEM images (c) EDS spectrum and (d) the diameter histograms and corresponding Gaussian fits of diameter of TNAs fabricated by anodising of a titanium sheet.

The FE-SEM micrograph of the Au NPs electroplated on TNAs electrodes with different magnifications was presented in fig. 3(a-b). It was evident that gold nanoparticles, high homogeneity and almost spherical shape, were assembled on the surface of the TNAs. Gold nanoparticles with diameter ranging from 86 to 90 nm dispersed on the nanotubes which was similar to the finding of Zhao et al [21]. Through EDS analysis, the deposition of gold nanoparticles on TNAs was confirmed from the EDS spectrum for gold (fig. 3(c)). The Au concentration was found close to 86 wt%.



Element	Intensity (c/s)	wt%.
O K	10.11	6.003
F K	2.82	1.169
Ti K	80.51	6.789
Au M	440.26	86.039

(c)
Fig. 3: Illustrative the surface morphology of Au NPs deposited on the TNAs at (a) low and (b) high magnification and (c) EDS spectrum.

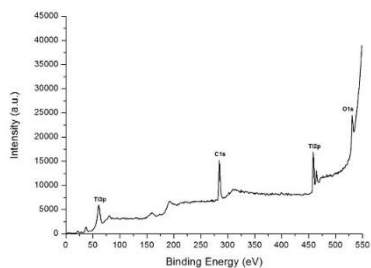
The XPS survey spectrum of the TNAs was presented in Fig. 4(a). As seen, the TNAs consisted of titanium (Ti2p), oxygen (O1s) and carbon (C1s). A very small quantity of C1s was due to the adsorption of carbon from the atmosphere. High resolution of Ti 2p of the TNAs was presented in Fig. 4(c). It can be seen that Ti2p_{3/2} and Ti2p_{1/2} peaks binding energies were located at 485.7 and 464.5 eV, respectively which are characteristic of Ti and O in TiO₂[22-25]. The XPS survey spectrum of the Au NPs/TNAs was presented in Fig. 4(b) referring to the elements gold, titanium, oxygen and carbon. The Au 4f (Fig. 4(d)) binding energies of 84.2 and 87.9 eV corresponded to Au species in the metallic state (Au⁰) [26-29]. The UV-Visible DRS spectra were used to investigate the optical absorption property of the samples in the range of 200-800 nm, as shown in Fig. 5. It has been observed that the TNAs displays the optical absorption edge located at 350 nm which in the UV light region. Au NPs/TNAs sample presented red-shifted absorption edge toward longer wavelength which located at about 500 nm and a strong absorption in the visible light region. This can be explained by the characteristic for localised surface plasmon resonance of Au NPs on the TNAs [30-32].

C. Photo catalytic activity

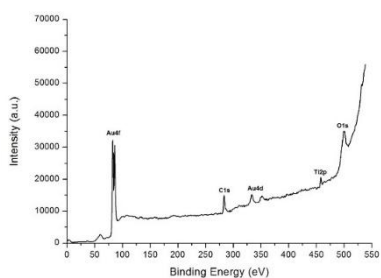
The photo catalytic activity was evaluated by the degradation of MB in an aqueous solution. The decolourisation of methylene blue was investigated under four different conditions: without any catalyst (blank), in the presence of catalyst of titanium sheet, TNAs and Au NPs/TNAs under visible light irradiation. Prior to initiation of the photo catalytic experiment (t=0), the initial concentration of MB (C₀) were equal for all the samples. The direct comparison of percent degradation of methylene blue with and without titanium dioxide as catalyst was shown in Fig. 6. For the blank experiment under visible light irradiation, the percent degradation of methylene blue was observed about 36%. It was apparent that using Au NPs/TNAs as a catalyst showed the highest photo catalytic

activity of 87% methylene blue degradation as compared to 41 and 72% for titanium sheet and TNAs, respectively in 48 hours.

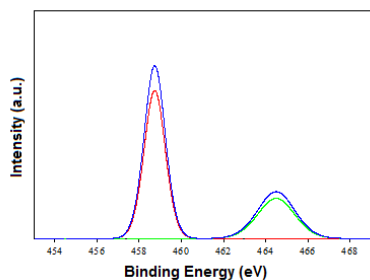
involves chemisorption, where the removal from a solution was due to physicochemical interactions between the two phases [33,34].



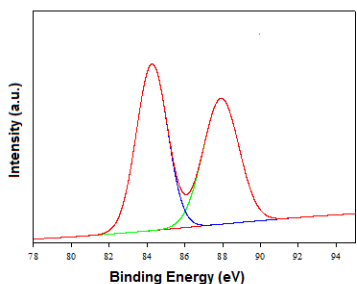
(a)



(b)



(c)



(d)

Fig 4: XPS survey spectra for (a) TNAs and (b) Au NPs/TNAs (c) Ti2p XPS photoelectron peak for TNAs and (d) Au4f XPS photoelectron peak for Au NPs/TNAs.

The pseudo first- order kinetic plot and the pseudo second-order kinetic plot were shown in Fig. 7. The relevant parameters derived by regressive analysis were listed in Table 2. The obtained regression values (R2) shown that pseudo second-order kinetics described the adsorption of methylene blue better than that of pseudo first-order kinetic model in all cases. The pseudo second-order kinetic model which the rate-limiting step was the surface adsorption that

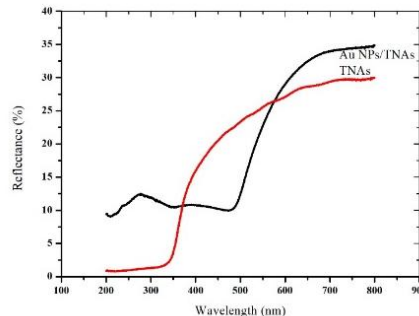


Fig. 5: UV-Vis reflectance spectra of TNAs and Au NPs/TNAs.

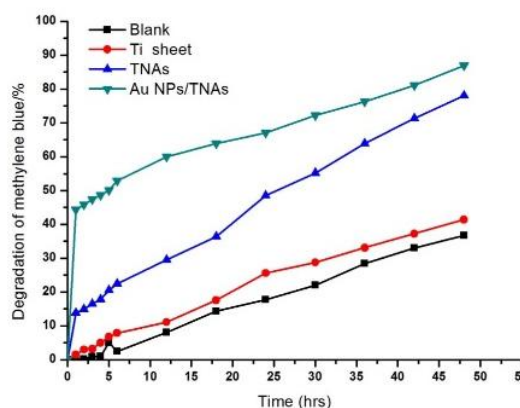


Fig. 6: Results of photo degradation of methylene blue under visible light.

An apparently increased photo catalytic activity was found for the TNAs catalyst under visible light irradiation. Many researchers have reported that the photocatalytic activity of titanium dioxide strongly depended on the preparation method as well as the post-treatment conditions. Increase surface hydroxyl content obviously influences to the photo activity of titanium dioxide. The increased hydroxyl groups on the TNAs will react with photo excited holes on the surface of TiO₂ and produce hydroxyl radicals, which in turn are powerful oxidants in the photocatalytic reaction and produce hydroxyl radicals, which in turn are powerful oxidants in the photo catalytic reaction [35-37].

The photo catalytic decomposition of methylene blue was enhanced by the deposited Au NPs on the TNAs as catalysts. There are three potential mechanisms that can contribute to drive photo catalytic reactions, namely, SPR-mediated charge injection mechanism, the near-field electromagnetic mechanism and scattering mechanisms. These mechanisms have been extensively reported in the literature regarding the higher activities on plasmonic photocatalysts under the irradiation of UV and a broad range of visible light. The mechanism of SPR based on the photo induced collective oscillators of electrons at the surface of Au nanoparticles. As a result of photo generated electrons, an increased local electromagnetic field is created.

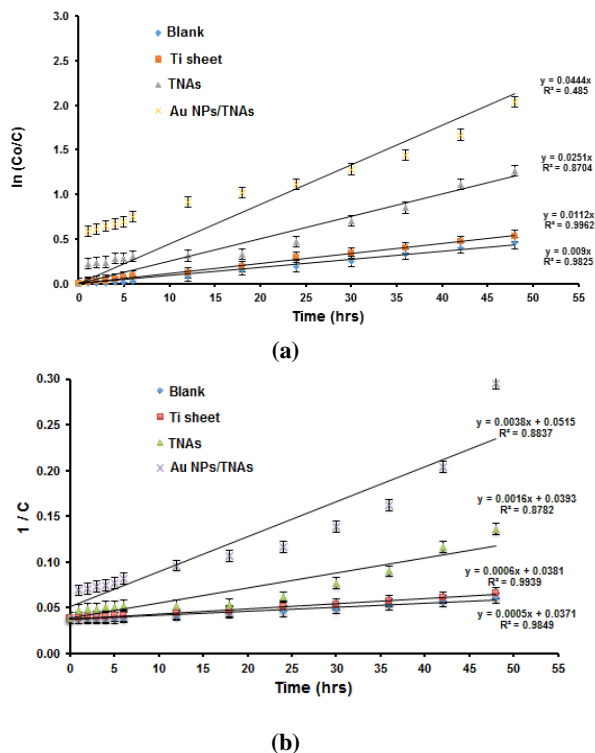


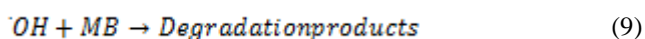
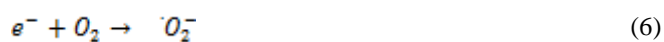
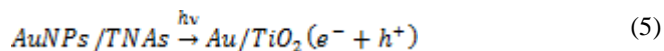
Fig. 7: Kinetic analysis (a) pseudo first-order and (b) pseudo second-order kinetics plots.

Table 2: Kinetic parameters of MB photo degradation using different catalysts.

Catalyst	% Degradation for 48 hours	Pseudo first-order		Pseudo second-order	
		k_1 (h^{-1})	R^2	k_2 (h^{-1})	R^2
Blank	36	0.0090	0.982	0.0005	0.984
Ti sheet	41	0.0112	0.996	0.0006	0.993
TNAs	72	0.0251	0.870	0.0016	0.878
Au NPs/TNAs	87	0.0444	0.485	0.0038	0.883

The interaction of the local electric field with TiO_2 induced the formation of charge carriers can reach the surface sites of the TiO_2 which increased the electron-hole separation [38-45]. Consequently the energy barrier will suppress the recombination reaction between the photo generated electrons and holes. Afterwards, the adsorbed oxygen molecules are trapped through formation of superoxide radical anions ($O_2^{\cdot-}$) then the superoxide radical anions ($O_2^{\cdot-}$) can further react with H^+ and the trapped electron to produce H_2O_2 in solution. The formed H_2O_2 will be transformed into hydroxyl radical (OH^{\cdot}) by capturing an electron on the surface of Au NPs/TNAs. Both hydroxyl radical (OH^{\cdot}) and superoxide radical ($O_2^{\cdot-}$) are very strong oxidising and they are able to decompose the organic molecules (MB) on the surface of the Au NPs/TNAs. The

photocatalytic reaction of AuNPs/TNAs, the formation of electrons and holes are summarised in the following equations [46,47]:



IV. CONCLUSION

Results demonstrated that Au NPs/TNAs have been productively synthesized by anodisation and electroplating process. FE-SEM, EDS and XPS data revealed the deposition of gold nanoparticles on titanium dioxide nanotube arrays. The Au NPs/TNAs exhibited the highest photocatalytic activity due to gold nanoparticles played a key role for the photocatalytic activity in degrading organic dyes in textile effluents. Therefore, potentially Au NPs/TNAs with higher visible light absorption and photocatalytic activity are promising material for organic pollutant degradation.

ACKNOWLEDGMENT

Financial support for this research was provided by Srinakharinwirot University under contract number 771/2558. Partial support was obtained from Graduate School, Srinakharinwirot University.

REFERENCES

- [1] A. Fujishima, and A. Honda, "Electrochemical photolysis of water at a semiconductor electrode," *Nature*, vol. 238, pp. 37-39, July 1972.
- [2] M.A. Lazer, S. Varghese, and S.S. Nair, "Photo catalytic water treatment by titanium dioxide: recent updates," *Catalysis*, vol. 2, pp. 572-601, Dec. 2012.
- [3] H. Lachheb, E. Puzenat, A. Houas, A. Ksibi, E. Elaloui, C. Guillard, and J.-M. Herrmann, "Photo catalytic degradation of various types of dyes (alizarin s, crocein orange g, methyl red, congo red, methylene blue) in water by UV-irradiated titania," *Applied Catalysis B: Environmental*, vol. 39, pp. 75-90, Nov. 2002.
- [4] M. Pelaez, N.T. Nolan, S.C. Pillai, M.K. Seery, P. Falaras, A.G. Kontos, P.S.M. Dunlop, J.W.J. Hamilton, A.J. Byrne, K. O'Shea, M.H. Entezari, and D.D. Dionysiou, "A review on the visible light active titanium dioxide photo catalysts for environmental applications," *Applied Catalysis B: Environmental*, vol. 125, pp. 331-349, August 2012.
- [5] P. Roy, S. Berger, and P. Schmuki, "TiO2 nanotubes: synthesis and applications," *Angew. Chem. Int. Ed.*, vol. 20, pp. 2904-2939, March 2011.
- [6] A. Zaleska, "Doped- TiO2: A review," *Recent Patents on Engineering*, vol. 2, pp. 157-164, Nov. 2008.

- [7] N.L. Wu, and M.S. Lee, "Enhanced TiO₂ photocatalysis by Cu in hydrogen production from aqueous methanol solution," *International Journal of Hydrogen Energy*, vol. 29, no. 15, pp. 1601–1605, Dec. 2004.
- [8] C.H. Lai, J.C. Juan, W.B. Ko, and S.B.A. Hamid, "An overview: recent development of titanium oxide nanotubes as photo catalyst for dye degradation," *International Journal of Photo energy*, Feb. 2014. Retrieved from <http://dx.doi.org/10.1155/2014/524135>
- [9] F. Pincella, K. Isozaki, and K. Miki, K. "A visible light-driven plasmonic photo catalyst," *Light: Science & Application*, vol. 3, pp. 1-6, Jan. 2014.
- [10] Z. Min, W. Juan, L. DanDan, and Y. Jiangjun Yang, "Enhanced visible light photocatalytic activity for TiO₂ nanotube array films by codoping with tungsten and nitrogen," *International Journal of Photo energy*, July 2013 Retrieved from <https://www.hindawi.com/journals/ijp/2013/471674/>
- [11] J. Schneider, M. Matsuoka, M. Takeuchi, J. Zhang, Y. Horiuchi, M. Anpo, and D.W. Bahnemann, "Understanding TiO₂ photocatalysis: mechanisms and materials," *Chemical Reviews*, vol. 114, pp. 9919-9986, Sep. 2014.
- [12] S. Benerjee, S.C. Pillai, P. Falaras, K.E. O'Shea, J.A. Byrne, and D.D. Dionysiou, "New insights into the mechanism of visible light photo catalysis," *Journal of Physical Chemistry Letters*, vol. 5, pp. 2543-2554, July 2014.
- [13] V. Subramanian, E.E. Wolf, and P.V. Kamat, "Catalysis with TiO₂/Gold Nanocomposites. Effect of metal particles size on the Fermi level equilibrium," *JACS*, vol. 126. pp. 49943-4950, March 2004.
- [14] Y. Tian, and T. Tatsuma, "Mechanisms and applications of plasmon-induced charge separation at TiO₂ films loaded with gold nanoparticles," *J. Am. Chem. Soc.*, vol. 127, pp. 7632-7637, April 2005.
- [15] A. Stevanovic, S. Ma, and J.T. Jr Yates, "Effect of gold nanoparticles on photo excited charge carriers in powdered TiO₂-long range quenching of photoluminescence," *J. Phys. Chem. C*. vol. 118, no. 36, pp. 21275-21280, August 2014.
- [16] S. Thongyoy, and A. Aeimbhu, "Synthesis of self-aligned titanium oxide nanotube arrays in ammonium fluoride-ethylene glycol electrolytes with different water contents," *Advanced Materials Research*, vol. 463-464, pp. 788-792, Feb. 2012.
- [17] C.J. Lin, Y.H. Yu, S.Y. Chen, and Y.H. Liou, "Anodic growth of highly ordered titanium oxide nanotube arrays: Effects of critical anodization factors on their photocatalytic activity," *World Academy of Science, Engineering and Technology*. Vol. 65, pp. 1094-1099, May 2010.
- [18] S.K. Kansal, and M. Chopra, "Photo catalytic degradation of 2,6-Dichlorophenol in aqueous phase using titania as a photo catalyst," *Engineering*. Vol. 4, pp. 416-420, August 2012.
- [19] S.S. Al-Shamali, "Photo catalytic degradation of methylene blue in the presence of TiO₂ catalyst assisted solar radiation," *Australian Journal of Basic and Applied Sciences*, vol. 7, no. 4, pp. 172-176, 2013.
- [20] L. Zou, Y. Luo, M. Hooper, and E. Hu, "Removal of VOCs by photo catalysis process using adsorption enhanced TiO₂-SiO₂ catalyst," *Chemical Engineering and Processing*, vol. 45, pp. 959–964, April 2006.
- [21] G. Zhao, Y. Lei, Y. Zhang, H. Li, and M. Liu, "Growth and favorable bioelectrocatalysis of multishaped nanocrystal Au in vertically aligned TiO₂ nanotubes for hemoprotein," *J. Phys. Chem. C*, vol. 112, pp. 14786-14795, August 2008.
- [22] J.F. Moulder, W.F. Stickle, P.E. Sobol, and K.D. Bomben, "Handbook of X-ray Photoelectron Spectroscopy," Perkin-Elmer Corporation. 1992
- [23] H. Park, H-G. Kim, and W-Y. Choi, "Characterizations of highly ordered TiO₂ obtained by anodic oxidation," *J. Trans Electr. Electron Mater*, vol. 11, pp. 112-115, June 2010.
- [24] J.H. Kim, S. Lee, and H.S. Im, "The effect of target density and its morphology on TiO₂ thin films grown on Si(100) by PLD," *Applied Surface Science*, vol. 151, no. 1-2, pp 6-16, Sep. 1999.
- [25] S. Zhu, S. Liang, Q. Gu, L. Xie, J. Wang, Z. Ding, and P. Liu, "Effect of Au supported TiO₂ with dominant exposed {0 0 1} facets on the visible-light photo catalytic activity," *Applied. Catalyst B: Environmental*, vol. 150, no. 119-120, pp. 146-155, May 2012.
- [26] J.F. Moulder, W.F. Stickle, P.E. Sobol, and K.D. Bomben, "Handbook of X-ray Photoelectron Spectroscopy," Perkin-Elmer Corporation, 1992.
- [27] V. Jovic, W.T. Chen, D. Sun-Waterhouse, M.G. Blackford, M. H. Idriss, and G.I.N. Waterhouse, "Effect of gold loading and TiO₂ support composition on the activity of Au/TiO₂ photocatalysts for H₂ production from ethanol–water mixtures," *Journal of Catalysis*, vol. 305, pp. 307-317, Sep. 2013.
- [28] A. Bumajdad, M. Madkour, Y. Abdel-Moneam, and M. El-Kemary, "Nanostructured mesoporous Au/TiO₂ for photocatalytic degradation of a textile dye: the effect of size similarity of the deposited Au with that of TiO₂ pores," *J. Mater. Sci*, vol. 49, no. 4, pp. 1743-1754, Nov. 2014.
- [29] M. Mrowetz, A. Villa, L. Prati, and E. Selli, "Effect of Au nanoparticles on TiO₂ in the photocatalytic degradation of an azo dye," *Gold Bulletin*, vol. 40, pp. 154-160, June 2007.
- [30] M.S. Hass, T. Amna, O-B. Yang, H.-C. Kim, and M-S. Khil, "TiO₂ nanofibers doped with rare earth elements and their photo catalytic activity," *Ceramics International*, vol. 38, pp. 5925-5930. Sep. 2012
- [31] A. Krukosk, J. Reszczynska, and A. Zaleska, Au-RE-TiO₂ nanocomposites: surface characteristic and photo activity. *Physicoche Ballanis, C.A.*, "Antenna theory analysis and design", 3rd edition, John Wiley and Son's Inc. New York, 2005.
- [32] *m. Probl. Miner. Process*, vol. 50, no. 2, pp. 551-561, Jan. 2014.
- [33] L. Wu, F. Li, Y. Xu, J.W. Zhang, G. Li, and H. Li, "Plasmon-induced photoelectrocatalytic activity of Au nanoparticles enhanced TiO₂ nanotube arrays electrodes for environmental remediation," *Applied Catalysis B: Environmental*, vol. 164, pp. 217-224, March 2015.
- [34] D. Robati, "Pseudo-second-order kinetic equations for modeling adsorption systems for removal of lead ions using multi-walled carbon nanotube," *Journal of Nanostructure in Chemistry*, vol. 3, no. 55, July 2013.
- [35] Y.H. Li, S. Wang, Z. Luan, J. Ding, C. Xu, and D. Wu, "Adsorption of cadmium(II) from aqueous solution by surface oxidized carbon nanotubes," *Carbon*, vol. 41, pp. 1057–1062, April 2003.

- [36] M. Zhang, J. Wu, D.D. Lu, and J. Yang, "Enhanced Visible Light Photo catalytic Activity for TiO₂ Nanotube Array Films by Codoping with Tungsten and Nitrogen," *International Journal of Photo energy*, 2013. Retrieved from <http://dx.doi.org/10.1155/2013/471674>
- [37] J.G. Yu, H.G. Yu, B. Cheng, M. Zhou, and X. Zhao, "Enhanced photo catalytic activity of TiO₂ powder (P25) by hydrothermal treatment," *Journal of Molecular Catalysis A*, vol. 253, no. 1-2, pp. 112-118, July 2006.
- [38] G.P. Dai, S.Q. Liu, S.T. Luo, X. Wang, and A.Z. Hu, "Hydrothermal treatment and enhanced photoelectrocatalytic activity of anatase TiO₂ nanotube arrays," *Chinese Journal of Inorganic Chemistry*, vol. 28, pp. 1617-1622, August 2012.
- [39] H. Wang, J.L. Faria, S. Dong, and Y. Chang, "Mesoporous Au/TiO₂ composites preparation, characterization, and photocatalytic properties," *Materials Science and Engineering B*, vol. 177, pp. 913-919, June 2012.
- [40] A. Bumajdad, M. Madkour, Y. Abdel-Moneam, and M. El-Kemary, "Nanostructured mesoporous Au/TiO₂ for photocatalytic degradation of a textile dye: the effect of size similarity of the deposited Au with that of TiO₂ pores," *J. Mater. Sci*, vol. 49, no. 4, pp. 1743-1754, Feb. 2014.
- [41] R. Amrollani, M.S. Hamdy, and G. Mul, "Understanding promotion of photocatalytic activity of TiO₂ by Au nanoparticles," *Journal of Catalysis*, vol. 319, pp. 194-199, Nov. 2014.
- [42] Y. Tian, and T. Tatsuma, "Mechanisms and applications of plasmon-induced charge separation at TiO₂ films loaded with gold nanoparticles," *J. Am. Chem. Soc.*, vol. 127, pp. 7632-7637, April 2005.
- [43] V. Subramanian, E.E. Wolf, and P.V. Kamat, "Catalysis with TiO₂/Gold Nanocomposites. Effect of metal particles size on the fermi level equilibrium," *J. Am. Chem. Soc.*, vol. 126, pp. 49943-4950, March 2004.
- [44] A. Stevanovic, S. Ma, and J.T. Jr. Yates, "Effect of gold nanoparticles on photo excited charge carriers in powdered TiO₂-long range quenching of photoluminescence," *J. Phys. Chem. C*, vol. 118, no. 36, pp. 21275-21280, August 2014.
- [45] D. Jose, C.M. Sorensen, S.S. Rayula, K.M. Shrestha, and K.J. Klabunde, "Au-TiO₂ nanocomposites and efficient photocatalytic hydrogen production under UV-Visible and visible light illuminations: a comparison of different crystalline forms of TiO₂," *International Journal of Photo energy*, 2013. Retrieved from <http://dx.doi.org/10.1155/2013/685614>
- [46] N. Pugazhenthiran, S. Murugesan, and S. Anandan, "High surface area Ag-TiO₂ nanotubes for solar/visible-light photocatalytic degradation of ceftriaxone sodium," *J. Hazardous Materials*, vol. 263, pp. 541-549, Dec. 2013.
- [47] S. Zhu, S. Liang, Q. Gu, L. Xie, J. Wang, Z. Ding, and P. Liu, "Effect of Au supported TiO₂ with dominant exposed {0 0 1} facets on the visible-light photocatalytic activity," *Applied. Catalyst B: Environmental*, vol. 150, no. 119-120, pp. 146-155, May 2012.
- [48] M. Zhou, J. Zhang, B. Cheng, and H. Yu, "Enhancement of Visible-Light Photocatalytic Activity of Mesoporous Au-TiO₂ Nanocomposites by Surface Plasmon Resonance," *International Journal of Photo energy*, 2012. Retrieved from <http://dx.doi.org/10.1155/2012/532843>